COMPARISON OF THE FAST SWEEPING AND FAST MARCHING METHODS FOR FIRST-ARRIVAL P-WAVE TRAVELTIME CALCULATION IN ATTENUATING VTI MEDIA

ZHENCONG ZHAO, JINGYI CHEN* and MENGXIU WANG

Seismic Anisotropy Group, Department of Geosciences, The University of Tulsa, Tulsa, OK 74104, U.S.A. jingyi-chen@utulsa.edu

ABSTRACT

Zhao, Z.C., Chen, J. and Wang, M.X., 2020. Comparison of the fast sweeping and fast marching methods for first-arrival P-wave traveltime calculation in attenuating VTI media. *Journal of Seismic Eploration*, 29: 403-424.

   First-arrival traveltime plays a crucial role in many geophysical applications such as static correction, tomography and prestack migration. Eikonal equation has been proven as an effective tool to calculate the first-arrival traveltime even in complex subsurface media. In attenuating media, eikonal equation can provide not only the information of first-arrival traveltime, but also amplitude decay. The real part of the complex-valued traveltime corresponds to seismic phase, while its imaginary part describes seismic attenuation due to energy absorption. Since the Fast Sweeping and Fast Marching methods have been considered as two effective eikonal equation solvers, it is necessary to compare them for the performances of calculating the complex-valued first-arrival P-wave traveltime in attenuating vertical transversely isotropic (VTI) media. The numerical tests show that the Fast Sweeping method is less time-consuming than the Fast Marching method, while having the same numerical accuracy.

KEY WORDS: eikonal equation, attenuation, transverse isotropic,
                Fast Sweeping method, Fast Marching method.

INTRODUCTION

First-arrival traveltime plays an important role in seismic migration and tomography (Lan and Zhang, 2013). The ray-tracing method and eikonal solution are two numerical schemes which are widely used in the calculation of first arrivals. In most cases, the traveltimes can be accurately and efficiently calculated by a ray-tracing method. However, the ray-traced traveltimes may sometimes not honor the actual first arrivals due to either a waveguide or shadow zone (Xu et al., 2006; Červený and Pšencík, 2009). Seismic rays may fail to penetrate through shadow zones (low velocity zone), and first arrivals in a waveguide may result from a complex interference phenomenon (Qin et al., 1992). In either case, the ray tracing method may be computationally expensive since the ray associated with the energy of the first arrival fails to be found. Without the influences of shadow zone and waveguide, the solutions of eikonal equations show the stability and applicability in complex media. Eikonal equations are derived from the high-frequency asymptotic wave equations and the first-arrival traveltimes satisfy the equations. Vidale (1988) proposed a finite-difference method to approximate the acoustic eikonal equation based on the idea of the wavefront propagation. However, the finite-difference method is unstable when the distribution of velocity changes rapidly (Qin et al., 1992). Sethian (1996) implemented the Fast Marching method based on entropy-satisfying upwind scheme, which is accurate and highly efficient for wavefront calculation. Since then, this method has been definitely applied to the traveltime calculation of seismic wave propagation (Alkhalifah and Fomel, 2001; Popovici and Sethian, 2002; Lan et al., 2012). The Fast Marching method assumes that the ray direction (the direction of energy propagation) is the normal direction of wavefront, which is only valid in isotropic media. Zhao (2005) proposed a Fast Sweeping method to calculate the numerical solution of the isotropic eikonal equation, which has been proven to be more robust than the Fast Marching method (Waheed et al., 2015).

Seismic anisotropy is widespread in the earth (Thomsen, 1986). Many geological structures (e.g., periodic sequences of thin layers, oriented cracks and parallel fractures) usually exhibit anisotropic properties which strongly affect seismic wave propagation. Such media can be described by transversely isotropic media. For the fractured reservoir characterization and source localization, it is necessary to calculate first arrivals in the presence of anisotropy (Schoenberg and Sayers, 1995; Tsvankin, 2012; Tsvankin and Grechka, 2011). Seismic traveltime calculation in an anisotropic medium has been studied by numerous researchers (Babuska and Cara, 1991; Kendall, 1994; Blackman et al., 1996). The Fast Marching and Fast Sweeping methods used to calculate the solution of eikonal equation in isotropic media are modified to apply to the anisotropic eikonal equation (Qian et al., 2007). Sethian and Vladimirsky (2003) proposed a modified Fast Marching algorithm to deal with anisotropic models. But the computational cost increases with the strength of anisotropy. Although Konukoglu et al. (2007)

and Cristiani (2009) incorporated velocity anisotropy into the Fast Marching algorithm to account for wave propagation in anisotropic media, it can only be applicable to the elliptical anisotropy. Waheed et al. (2015) proposed an iterative, Fast Sweeping algorithm to solve the anisotropic eikonal equation. However, this algorithm suffers from source-singularity problem due to the source-point initial condition, which may result in a significant increase of the truncation error in the traveltime calculation near the source. This can further result in the convergence of an inaccurate solution (Waheed and Alkhalifah, 2017). Waheed and Alkhalifah (2017) solved the source-singularity problem effectively by using the factorization method proposed by Fomel et al. (2009). The traveltimes are factorized into two multiplicative factors, one is used to capture the source singularity and the other can be regarded as the background solution.

Seismic attenuation is another important component of wave propagation in subsurface media (Hao and Alkhalifah, 2017a, 2017b). Formations or aligned fractures that show velocity anisotropy are often characterized by even stronger attenuation anisotropy (Bai et al., 2017). Many laboratory experiments have demonstrated that attenuation anisotropy may help to estimate the orientation of layered formations or the presence of laminae in the rocks (Chichinina et al., 2006; Guo and McMechan, 2017; Bai and Tsvankin, 2019). The time-harmonic wave traveltime in the viscoacoustic medium is generally complex-valued and is governed by the complex eikonal equation (Červený, 2005). The real part of complex-valued eikonal equation has the same form to the real eikonal equation in nonattenuating media. From the ray theory, the real part of the complex-valued traveltime from a time-harmonic ray describes the wave phase, and the imaginary part corresponds to the attenuation due to the energy absorption in viscoacoustic media (Hao and Alkhalifah, 2017a; Hao and Alkhalifah, 2019). Zhu and Tsvankin (2006) presented a Thomsen-style notation to describe the anisotropy of attenuation coefficient for plane waves in attenuative anisotropic media. The introduction of Thomsen-style notation leads to the concise form of eikonal equation in viscoacoutic media. They found that the attenuation coefficient of quasi P-wave A_{p0} is almost independent of the quasi S-wave attenuation coefficient A_{s0} and the impact of the S-wave velocity v_{s0} on the traveltime is weak and negligible. Thus, Hao and Alkhalifah (2017a) derived an acoustic eikonal equation using the acoustic approximation in attenuative VTI media.

Although the complex-valued eikonal equation shows a similar form as the real eikonal equation in nonattenuative media, it is hard to find the exact solution to the complex eikonal equation. Numerical schemes (e.g., the Fast Sweeping method and the Fast Marching method) widely used in the traveltime calculation for the nonattenuative medium, cannot be directly applied to the complex-valued eikonal equations since they are required to update the traveltime along the orientation of wavefront propagation by choosing the minimum of traveltimes in a heap. Selecting the minimum

value is also not valid for complex numbers. Hao and Alkhalifah (2017a) presented a perturbation method to approximate the complex-valued traveltime from the eikonal equation for the homogeneous attenuative VTI medium, and the shanks transform was adopted to accelerate the convergence of the series decomposed from the complex eikonal equation with respect to the perturbation parameters. Based on the perturbation method, they applied the modified Fast Marching scheme to calculate the solution of the complex-valued eikonal equation in inhomogeneous attenuative VTI media. Hao et al. (2018) implemented the Fast Sweeping method to calculate the solution of the complex-valued eikonal equation in attenuating VTI media.

The main goal of this paper is to compare the Fast Marching method and the Fast Sweeping method in term of accuracy, efficiency and stability in attenuative VTI media, in which the symmetry of the attenuation waves is the same as that of the phase velocity. The rest of this paper is organized as follows. First, we apply the perturbation method to the complex-valued eikonal equation in attenuative VTI media and decompose the complex form into two simpler expressions, which govern the real and imaginary parts of the complex-valued traveltime, respectively. Then, we solve the two simpler equations successively by using the Fast Sweeping method and the Fast Marching method. Two numerical tests are carried out to compare the two methods with respect to accuracy, efficiency and stability. Finally, we conclude that the Fast Sweeping method is as accurate and stable as the Fast Marching method but more efficient.

THEORY

The acoustic eikonal equation for 2D (x, z) attenuative VTI media is expressed as (Hao and Alkhalifah, 2017a):

$$At_x^2 + Bt_z^2 + Ct_x^2 t_z^2 = 1 \quad , \tag{1}$$

where t is the complex-valued traveltime, and and t_x and t_z denote the first-order derivatives of traveltime with respect to the directions x and z, respectively; The coefficients A, B and C are expressed through the medium properties as:

$$A = v_n^2 \left(1 + 2\eta\right)\left(1 - 2ik_q\left(1 + \varepsilon_Q\right)\right),$$

$$B = v_{P0}^2 \left(1 - 2ik_q\right),$$

$$C = \frac{v_{P0}^2}{v_n^2}\left(\left(1 - 2ik_q\right)v_n^2 - ik_q\delta_Q v_{P0}^2\right)^2 - v_{P0}^2 v_n^2\left(1 + 2\eta\right)\left(1 - 2ik_q\right)\left(1 - 2ik_q\left(1 + \varepsilon_Q\right)\right),$$

with

$$k_q = \frac{A_{P0}}{1 - A_{P0}^2},$$

where i represents the imaginary unit; ε_Q and δ_Q are the Thomsen-style parameters for attenuation anisotropy introduced by Zhu and Tsvankin (2006); ε_Q is the fractional difference between the horizontal and vertical attenuation coefficients, and δ_Q is the second-order derivative of the attenuation coefficient A_p with respect to the phase angle of homogeneous plane quasi P-waves along the vertical direction. Note that ε_Q and δ_Q are believed to be predominantly negative. A_{p0} is the wavenumber-normalized attenuation coefficient of the vertically propagating P-wave, hereafter referred to as the P-wave vertical attenuation coefficient, for brevity.; v_{p0} and v_n are the P-wave velocity in the symmetry-axis direction and normal moveout velocity, respectively; and $\eta = (\varepsilon - \delta)/(1 + 2\delta)$ is the anellipticity parameter, where ε and δ are Thomsen anisotropy parameters (Thomsen, 1986).

Perturbation method

According to Alkhalifah (2000) and Hao and Alkhalifah (2017a), the perturbation method can be used to decompose a complex-valued equation into an infinite number of relatively simple equations by identifying a small parameter [e.g., k_q in eq. (1)] or several parameters and setting these parameters to zero. Thus, the complex-valued equation can be solved. Here, we choose k_q as the small parameter to decompose eq. (1) into two simple equations. Since i and k_q always appear in the product form in the eikonal equation, the two decomposed equations from the complex-valued equation represent the real part and imaginary part of complex-valued eikonal equation, respectively. Thus, the left part of the eq. (1) can be expressed as:

$$F\left(t,k_q\right)=1 \quad .$$

$$(2)$$

The perturbation parameter l is introduced to scale k in eq. (2),

$$F\left(t,lk_q\right)=1 \quad .$$

$$(3)$$

The first-order perturbation solution of eq. (2) is defined as:

$$t = t_0 + ilt_1 \quad ,$$

$$(4)$$

where t_0 and t_1 denote the zero-th and first-order traveltime coefficients, respectively. They also represent the real part and imaginary part of the complex-value traveltime, respectively.

We expand eq. (3) around $l = 0$, and obtain

$$F\left(t,ik_q\right)= F\left(t,0\right)+ilF_1\left(t,0\right),$$

$$(5)$$

where

$$F\left(t,0\right)= v_n^2\left(1+2\eta\right)t_{0x}^2 + v_{p0}^2 t_{0z}^2 - 2\eta v_n^2 v_{p0}^2 t_{0x}^2 t_{0z}^2,$$

$$F_1\left(t,0\right)= v_n^2\left(1+2\eta\right)t_{0x}t_{1x} + v_{p0}^2 t_{0z}t_{1z} - 2\eta v_n^2 v_{p0}^2\left(t_{0z}t_{1z}t_{0x}^2 + t_{0x}t_{1x}t_{0z}^2\right)-f_1,$$

$$f_1 = k\left(1+\varepsilon\right)v_n^2\left(1+2\eta\right)t_{0x}^2 + kv_{p0}^2 t_{0z}^2 + k\left(2v_n^2 v_{p0}^2 + \delta_Q v_{p0}^4 -\left(2+\varepsilon_Q\right)\left(1+2\eta\right)v_n^2 v_{p0}^2\right)t_{0x}^2 t_{0z}^2$$

In eq. (5), $F_1\left(t,0\right)$ denotes the first derivative of F with respect to the perturbation parameter l at $l = 0$. Since the right side of eq. (3) is equal to unity, which is a real number, we should have the following relationship

$$F\left(t,0\right)=1 \quad ,$$

$$(6a)$$

$$F_1\left(t,0\right)= 0.$$

$$(6b)$$

Factorization method

To solve eq. (6a), Waheed et al. (2015) proposed a modified Fast Sweeping algorithm to get the accurate solution, and applied the factorization method to address the source-singularity problem. For the multiplicative factorization, the real part of the traveltime is factorized into:

$$t_0 = T_0\tau_0 \quad , \tag{7}$$

where T_0 denotes the analytical solution of eq. (6a) for homogeneous VTI media, which overcomes the source singularity and τ_0 is an unknown factor which is smooth in the vicinity of the source position. The spatial traveltime derivatives are expressed as

$$t_{0x} = T_{0x}\tau_0 + T_0\tau_{0x} \ , \tag{8a}$$
$$t_{0z} = T_{0z}\tau_0 + T_0\tau_{0z} \ . \tag{8b}$$

By substituting eqs. (8a) and (8b) into (6a), we find the factored zeroth-order governing equation for the multiplicative factorization:

$$v_n^2(1+2\eta)\left(\tau_{0x}T_0 + T_{0x}\tau_0\right)^2 + v_{p0}^2\left(\tau_{0z}T_0 + T_{0z}\tau_0\right)^2 = f(\tau_0) \ , \tag{9}$$

where

$$f(\tau_0) = 1 + 2\eta v_n^2 v_{p0}^2 \left(\tau_{0x}T_0 + T_{0x}\tau_0\right)^2 \left(\tau_{0z}T_0 + T_{0z}\tau_0\right)^2 \ .$$

According to Luo and Qian (2012), T_0 may overcome the source singularity, while the function τ_0 is smooth near the source. The accurate calculation on τ_0 is crucial to find the accurate t_0. Here, T_0 is regarded as the solution of eq. (6a) in homogeneous case

$$v_{ns}^2(1+2\eta)T_{0x}^2 + v_{ps}^2 T_{0z}^2 = f(\tau_0) \ , \tag{10}$$

where $v_{ns} = v_n(x_s, z_s)$ and $v_{ps} = v_{p0}(x_s, z_s)$. (x_s, z_s) is the source location. The analytical solution of eq. (10) is given as:

$$T_0(x,z) = \sqrt{a(x-x_s)^2 + b(z-z_s)^2} \quad , \tag{11}$$

where

$$a = \frac{f(\tau_0)}{v_{ns}^2(1+2\eta)} \ ,$$

$$b = \frac{f(\tau_0)}{v_{ps}^2} \ .$$

By analogy with eq. (7), the imaginary part of the traveltime is given as:

$$t_1 = T_1\tau_1 \quad . \tag{12}$$

The spatial derivatives are expressed as:

$$t_{1x} = T_{1x}\tau_1 + T_1\tau_{1x} \quad , \tag{13a}$$

$$t_{1z} = T_{1z}\tau_1 + T_1\tau_{1z} \quad . \tag{13b}$$

Thus, the first-order governing equation can be written as:

$$v_n^2(1+2\eta)t_{0x}(T_{1x}\tau_1 + \tau_{1x}T_1) + v_{p0}^2 t_{0z}(T_{1z}\tau_1 + \tau_{1z}T_1) = g(\tau_1) \quad , \tag{14}$$

where

$$g(\tau_1) = f_1 + 2\eta v_n^2 v_{p0}^2 \left(t_{0z}(T_{1z}\tau_1 + T_1\tau_{1z})t_{0x}^2 + t_{0x}(T_{1x}\tau_1 + T_1\tau_{1x})t_{0z}^2\right) \quad .$$

The analytical solution of the first-order governing equation can be obtained

$$T_1 = \frac{a_1(x-x_s)^4 + b_1(x-x_s)^2(z-z_s)^2 + c_1(z-z_s)^4}{T_0^3} \quad , \tag{15}$$

where

$$a_1 = \frac{k(1+\varepsilon_Q)f^2(\tau_0)}{v_{ns}^4(1+2\eta)^2} \quad ,$$

$$b_1 = \frac{k(2v_{ns}^2(1+2\eta)+\delta_Q v_{ps}^2)f^2(\tau_0)}{v_{ns}^4(1+2\eta)^2 v_{ps}^2} \quad ,$$

$$c_1 = \frac{kf^2(\tau_0)}{v_{ps}^4} \quad .$$

Luo and Qian (2012) proposed a Fast Sweeping scheme to calculate τ_0 in eq. (9) based on eq. (11). On a rectangular grid with grid size h, for a grid point c, we discretize eq. (9) on four triangles with an common vertex c (Fig. 1).
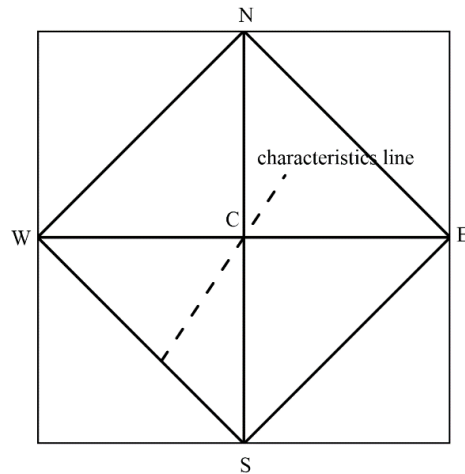

Fig. 1. Rectangular mesh and characteristics line.

For the triangle Δwcs, the expressions of τ_{0x} and τ_{0z} can be written as:

$$\left(\tau_{0x},\tau_{0z}\right) \approx \left(\frac{\tau_0(c)-\tau_0(w)}{h}, \frac{\tau_0(c)-\tau_0(s)}{h}\right) \quad . \tag{16}$$

By substituring eq. (16) into eq. (9), a quadratic equation in terms of τ_0 can be obtained

$$A'\tau_0^2 - 2B'\tau_0 + C' = 0 \quad , \tag{17}$$

where

$$A' = v_n^2\left(1+2\eta\right)m^2 + v_{p0}^2 n^2,$$
$$B' = v_n^2\left(1+2\eta\right)m\alpha + v_{p0}^2 n\beta,$$
$$C' = v_n^2\left(1+2\eta\right)\alpha^2 + v_{p0}^2\beta^2 - f\left(\tau_0\right),$$
$$m = T_{0x} + \frac{T_0}{h}, \quad n = T_{0z} + \frac{T_0}{h},$$
$$\alpha = \frac{T_0\tau(w)}{h}, \quad \beta = \frac{T_0\tau(s)}{h}.$$

If $\Delta = \left(2B'\right)^2 - 4A'C' \geq 0$, the candidate values of τ_0 can be solved from eq. (17). We denote this candidate value as $\tau_0^c(c)$ at the grid point c. Thus, for four triangles with a common vertex c, four quadratic equations in terms of τ_0 can be obtained. The acceptable candidate value should be real and satisfies the causality condition (Waheed et al., 2015). According to the causality condition, the characteristic line passing through the common vertex c should be between the two edges of each triangles. If no candidate value satisfies the causality condition or $\Delta < 0$, for triangle ∇wcs, the characteristic line passes through the common point c along two edges. For instance, if the characteristic line propagates along $\mathbf{wc}$, the derivative of eq. (9) with respect to t_{0z} should be zero, which yields $T_{0z}\tau_0 + T_0\tau_{0z} = 0$. By substituting this relationship into eq. (9), the viscosity solution for the triangle ∇wcs is given as:

$$\tau^c(c) = \frac{T_0(c)\tau_0(w) + h\sqrt{\dfrac{1}{v_n^2\left(1+2\eta\right)}}}{T_0(c) + T_{0x}(c)\left(x_c - x_w\right)} \quad . \tag{18}$$

For every grid point, at least four candidate values of τ_0 can be calculated and only the minimum value will be selected. Similar treatments as eqs. (16)-(18), the factorization method can also be applied to the first-order governing equation to tackle with source-singularity problem. For triangle ∇wcs, the expressions of τ_{1x} and τ_{1z} can be written as

$$\left(\tau_{1x}, \tau_{1z}\right) \approx \left(\frac{\tau_1(c) - \tau_1(w)}{h}, \frac{\tau_1(c) - \tau_1(s)}{h}\right) . \tag{19}$$

By substituting eq. (19) into eq. (14), the following expression in terms of τ_1 can be obtained

$$v_n^2\left(1 + 2\eta\right)t_{0x}\left(T_{1x}\tau_1 + T_1\frac{\tau_1 - \tau_1(w)}{h}\right) + v_{p0}^2 t_{0z}\left(T_{1z}\tau_1 + T_1\frac{\tau_1 - \tau_1(s)}{h}\right) = g_1. \tag{20}$$

The solution of eq. (20) at the grid point c can be obtained in the form:

$$\tau_1^c(c) = \frac{g_1 + v_n^2\left(1 + 2\eta\right)t_{0x}\dfrac{\tau_1(w)T_1}{h} + v_{p0}^2 t_{0z}\dfrac{\tau_1(s)T_1}{h}}{v_n^2\left(1 + 2\eta\right)t_{0x}\left(T_{1x} - \dfrac{T_1}{h}\right) + v_{p0}^2 t_{0z}\left(T_{1z} - \dfrac{T_1}{h}\right)} . \tag{21}$$

Similar to the candidate value of τ_0, τ_1^c is also required to satisfy the causality condition. Otherwise, we suppose that the characteristic line is along one of the edges of the triangles. If it propagates along the edge **wc**, the derivative of eq. (14) to t_{1z} should be equal to zero (Luo and Qian, 2012). Thus, $v_{p0}^2 t_{0z} = 0$. Substituting this relationship into eq. (20) yields

$$\tau_1^c = \frac{\dfrac{g_1 h}{v_n^2\left(1 + 2\eta\right)t_{0x}\left(T_{1x} - \dfrac{T_1}{h}\right)} + T_1\tau_1(w)}{T_{1x}h + T_1} . \tag{22}$$

The candidate value along the another edge of this triangle can be calculated in the same way by assuming $v_n^2\left(1 + 2\eta\right)t_{0x} = 0$. For a grid point c, at least four candidate values of τ_1 can be derived and the minimum value will be chosen.

ALGORITHM

Fast Sweeping method

Waheed et al. (2015) presented an iterative Fast-Sweeping-based eikonal solver in anisotropic media which can be applied to the zeroth-order governing equation. We combine this algorithm with the complex-valued eikonal equation. The steps of the modified fast sweeping method are as follows:

1) Discretization. The first-order finite-difference expressions for the spatial derivatives of factors τ_0 and τ_1 are given by

$$\tau_{k,x} = \left(\frac{\tau_k^{i,j} - \tau_{k,x\min}}{h} \right) s_x, \quad \tau_{k,z} = \left(\frac{\tau_k^{i,j} - \tau_{k,z\min}}{h} \right) s_z, \quad k = 0,1 \quad , \quad (23)$$

where $i = 2,3,...,I-1$, $j = 2,3,...,J-1$. h is the grid size; $\tau_{i,j}$ represents the value of unknown factor τ at the grid point (i,j); $\tau_{x\min}$ and $\tau_{z\min}$ denote the smaller values of neighboring nodes in the x and z directions, respectively. In other words, for the multiplicative factorization, the expressions of τ_x and τ_z are given by

$$\tau_{k,x\min} = \begin{cases} \tau_k^{i+1,j}, & if \tau_k^{i+1,j} T_0^{i+1,j} < \tau_k^{i-1,j} T_0^{i-1,j} \\ \tau_k^{i-1,j} & else \end{cases} ,$$

$$\tau_{k,z\min} = \begin{cases} \tau_k^{i,j+1}, & if \tau_k^{i,j+1} T_0^{i,j+1} < \tau_k^{i,j-1} T_0^{i,j-1} \\ \tau_k^{i,j-1} & else \end{cases} , \quad (24)$$

where s_x and s_z are parameters used to control the directions of the first-order derivatives (τ_x and τ_z).

$$s_x = \begin{cases} +1 & if \tau_{0,x\min} = \tau_0^{i-1,j} \\ -1 & else \end{cases}, \quad s_z = \begin{cases} +1 & if \tau_{0,z\min} = \tau_0^{i,j-1} \\ -1 & else \end{cases}. \quad (25)$$

2) Initialization. The real and imaginary parts of the complex-valued traveltimes t_0 and t_1 at the source location vanish, while the rest of the computational domain can be initialized with a large positive value. As a

result, for the multiplicative factorization, both τ_0 and τ_1 at the source node can be initialized with unity.

3) Calculate T_0 and T_1 analytically. T_0 and T_1 are the solutions of eqs. (9) and (14) for the homogenous case, respectively. After step 2), we evaluate T_0 and T_1 for the whole domain using eqs. (11) and (15), respectively.

4) Calculate τ_0 iteratively. After step 3), τ_0 of the whole domain can be calculated by solving eq. (17) or (18) and sweeping the whole domain repeatedly is implemented by the following order

$$
\begin{aligned}
&(1)\, i = 1:I,\, j = 1:J, \quad (2)\, i = 1:I,\, j = J:1, \\
&(3)\, i = I:1,\, j = 1:J, \quad (4)\, i = I:1,\, j = J:1,
\end{aligned}
\tag{26}
$$

For each grid node of the computational domain, the candidate value of τ_0 can be solved by eq. (17) and denoted by $\tau_{0i,j}^c$. Then $\tau_0^{i,j}$ will be updated if it satisfies the causality condition and minimum traveltime criterion. If this value does not meet the causality condition, $\tau_{0i,j}^c$ should be calculated from eq. (18) and then one needs to check if it meets the minimum traveltime criterion discretized as:

$$
\tau_{0i,j}^{new} = \begin{cases} \tau_{0i,j}^c, & if\, \tau_{0i,j}^c T_{0i,j} < \tau_{i,j}^{old} T_{0i,j} \\ \tau_{0i,j}^{old}, & else \end{cases}.
\tag{27}
$$

After updating the value of τ_0 in the whole domain, the real part of the complex-valued traveltime t_0 and f_1 in eq. (5) can be obtained by eqs. (7) and (5), respectively.

5) Update $f(\tau_0)$. After evaluating τ_0 at each point of the whole computational domain, $f(\tau_0)$ value at each node of the domain can be updated by solving the right-hand side of eq. (9). Noticed that at the first iteration, $f(\tau_0)$ is initialized with unity at each point of the whole computational domain.

6) Calculate τ_1 iteratively. Thus, for each grid point, once t_0 has been obtained in step 4), the derivatives of t_0 with respect to x and z axes, namely t_{0x} and t_{0z}, can be approximated using the first-order difference operator. Substituting these derivatives into eq. (21), the candidate value of

τ_1 can be derived and denoted as $\tau_{1i,j}^c$. Thus, the τ_1 for the whole domain can be calculated by solving eqs. (21) or (22) and sweeping the whole domain repeatedly can be done on the order in step 3). Then $\tau_1^{i,j}$ will be updated if the candidate value satisfies the causality condition and minimum traveltime criterion. If this value does not meet the causality condition, $\tau_{1i,j}^c$ should be calculated from eq. (22); next, it is necessary to check if it meets the minimum traveltime criterion.

7) Update $g(\tau_1)$ and repeat. After evaluating τ_1 at each points, $g(\tau_1)$ value at each node of the domain can be updated by solving the right-hand side of eq. (14). Notice that at the first iteration, $g(\tau_1)$ is initialized with f_1 at each point of the whole computational domain. Then repeat steps (3)-(6) until the result converges to the correction solution.

Fast Marching method

Here, we apply the Fast Marching method to calculate the first-arrival traveltime based on the complex-valued eikonal equation. Sethian (1996) used the sets *Far, Close* and *Alive* to descibe the status of grid points of the whole domain. The modified Fast Marching method is summarized as follows:

1) Same as in the Fast Sweeping algorithm, step 1).

2) Initialization. The unknown factors τ_0 and τ_1 at the source location are initialized with unity, while the rest of the points in the whole computational domain are set to a large number. Tag points in the initial conditions as *Alive*. Then tag as *Close* for the neighbouring points of the point in *Alive*. Finally, tag as *Far* for all rest grid points.

3) Same as in the Fast Sweeping algorithm, step 3).

4) Compute the τ_0 values of grid points in *Close* from eq. (17) or (18). If the new candidate value τ_0^c meets the minimum traveltime criterion, t_0 of the points can be calculated from eq. (7). Only the smallest value among these points will be tagged as *Alive*, and its neighboring points not in *Alive* will be tagged as *close*. Repeat this step until the *Far* is null. Thus, the t_0 values are updated for the whole computational domain. After calculating

the spatial derivatives of t_0 with respect to x and z, the value of f_1 can be obtained.

5) Same as in the Fast Sweeping algorithm, step 5).

6) Compute τ_1 values of grid points in *Close* from eq. (21) or (22). If the new candidate value τ_1^c meets the minimum traveltime criterion, t_1 of the points can be calculated from eq. (12). Among these points, only the point with the smallest value will be tagged as *Alive*, and its neighboring points not in Alive will be tagged as *close*. Repeat this step until the *Far* is null.

7) Same as the Fast Sweeping algorithm, step 7).

NUMERICAL TESTS

To carry out the comparison of the Fast Marching and Fast Sweeping methods, we first test two methods with the analytical solutions [eqs. (11) and (15)] in a homogenous attenuative VTI medium. Then, the SEG/Hess attenuative VTI model is used to further test the accuracy, efficiency and stability of the two numerical methods in complex media.

Homogeneous attenuating VTI model (Model 1)

The model size is $1.5km \times 1.5km$, and the grid size is 5 m. The P-wave vertical attenuation coefficient A_{p0} is 0.025, the Thomsen's parameter δ is 0.1, the Thomsen-style parameters ε_q and δ_q for attenuation anisotropy are -0.3 and 0.98, respectively (Zhu and Tsvankin, 2006), the anellipticity parameter η is 0.16, the P-wave vertical velocity v_p and normal moveout velocity v_n are $3km/s$ and $3.286\,km/s$, respectively. The source is located at the center of the model. Fig. 2 shows the real parts of the complex-valued traveltimes obtained with (a) the Fast Marching method (thick dashed line), (b) the Fast Sweeping method (thick dashed line) and the analytical solution (solid line). Fig. 3 shows the imaginary parts of the complex-valued traveltimes obtained with (a) the Fast Marching method (thick dashed line), (b) the Fast Sweeping method (thick dashed line) and the analytical solution (black solid line). In Fig. 2, we can see that the real parts of traveltimes calculated from both numerical methods have the same values

as those obtained from the analytical solution. In Fig. 3, one can observe that the errors between the imaginary parts of the traveltimes calculated from both numerical methods and the analytical solution increase, as the distance from the source increases.
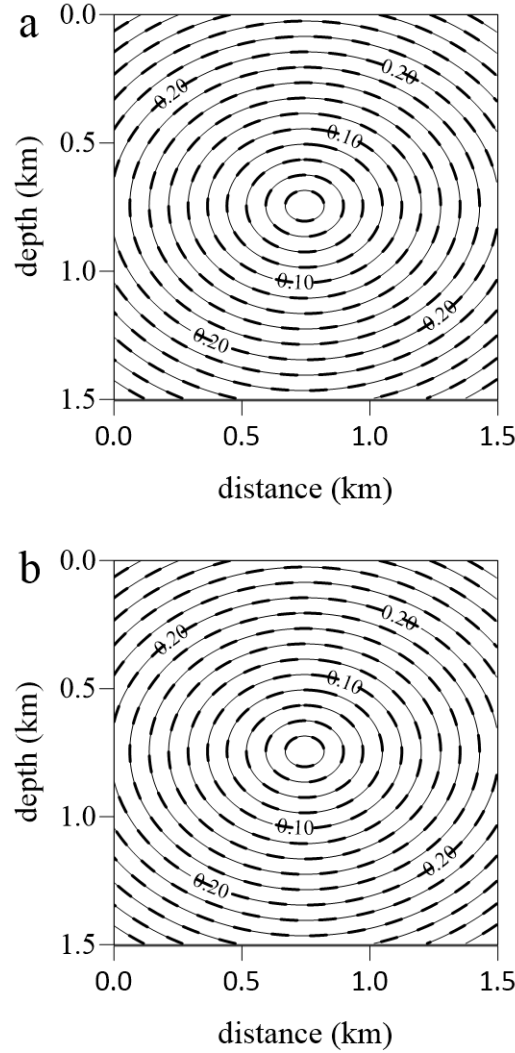

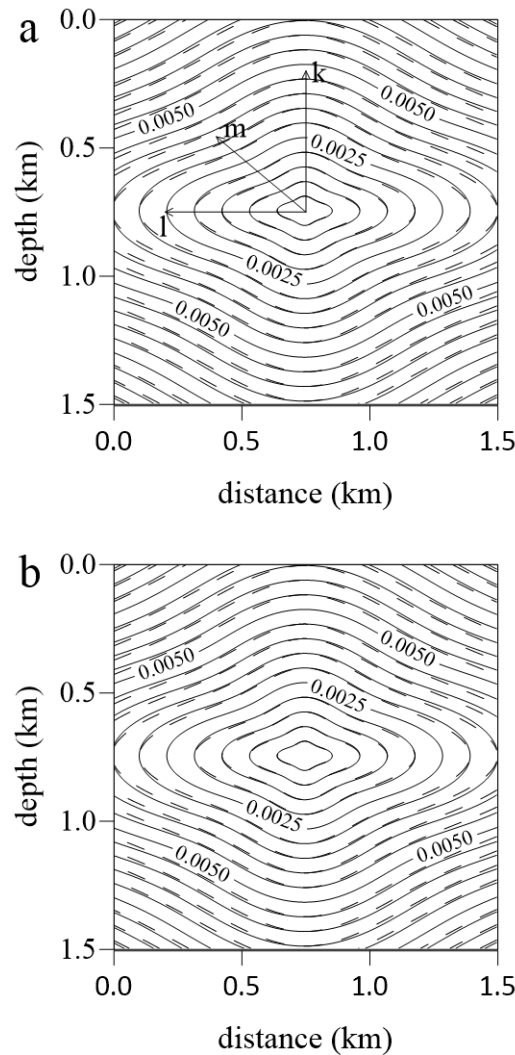Fig. 2. Real parts of the complex-valued traveltimes calculated from (a) the Fast Marching method and (b) the Fast Sweeping method for Model 1.

According to the studies on seismic attenuation (Zhu and Tsvankin, 2006; Vavryčuk, 2007, 2010; Hao and Alkhalifah, 2017a), the exponential term $e^{-\omega t_1(\mathbf{x})}$ is to control the amplitude decays of seismic waves, where ω, t_1 and $\mathbf{x}$ stand for the angular frequency, value of the imaginary part of traveltime and distance away from the source, respectively. For the same travel distance from source, the larger value of the imaginary part of traveltime t_1 indicates the stronger seismic attenuation. In Fig. 3a, lines k, m

and l represent the 0°, 40° and 90° deviated from the upward vertical direction, respectively. We can observe that the largest and smallest values of t_1 are along directions m and l for the same travel distance from source, respectively, which indicates the maximum and minimum seismic attenuations are along the angles 40° and 90°, respectively. We can also see that the seismic attenuation in the vertical direction (line k direction) is stronger than that in the horizontal direction (line l direction), which can be verified by the Thomsen-style notation $\varepsilon_Q = \dfrac{Q_{33} - Q_{11}}{Q_{33}}$. The negative ε_Q (-0.3 used in this model) means that the value of the quality factor Q_{33} (vertical direction) is smaller than Q_{11} (horizontal direction). Note the seismic quality factor is inversely proportional to the strength of the attenuation.

Fig. 3. Imaginary parts of the complex-valued traveltimes calculated from (a) the Fast Marching method and (b) the Fast Sweeping method for Model 1.
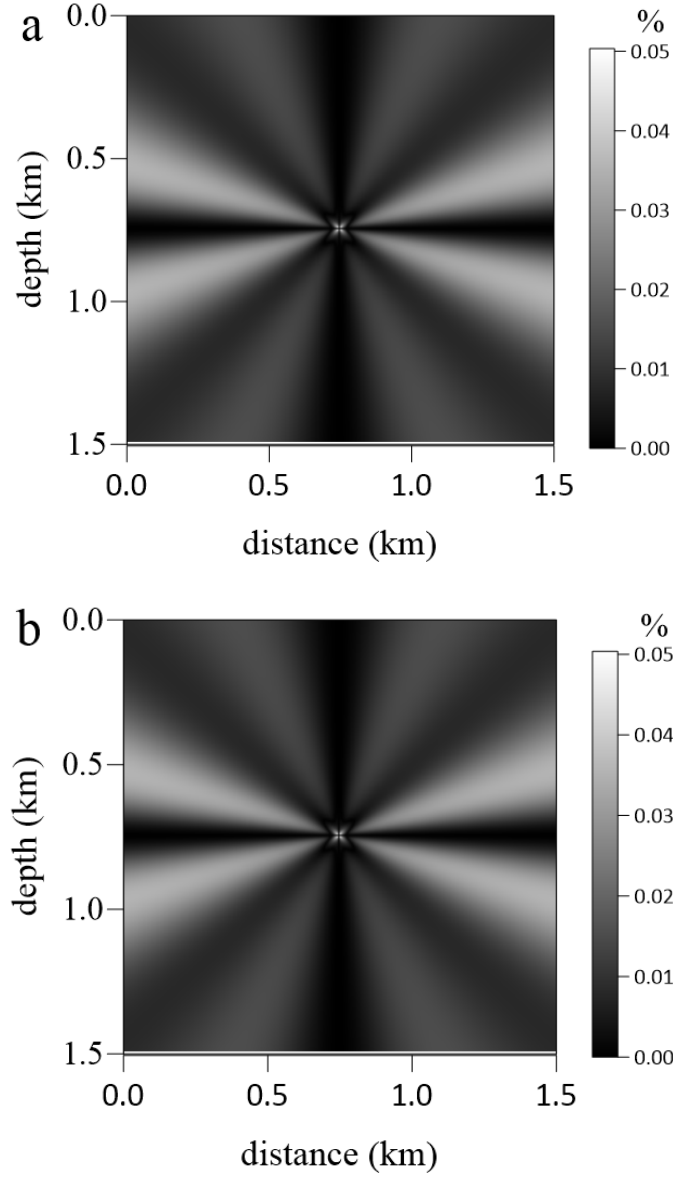
Fig. 4. Errors in the imaginary parts of the complex-valued traveltimes computed with the (a) Fast Marching method and (b) the Fast Sweeping method.

Fig. 4 shows the errors the of imaginary parts of the complex-valued traveltimes calculated from the Fast Marching method (a) and the Fast Sweeping method (b), respectively. The errors are calculated as $\dfrac{|T_{ex} - T_{ns}|}{T_{ex}}$, where T_{ex} and T_{ns} are the exact solution (Hao and Alkhalifah, 2017a) and the numerical solution, respectively. From Fig. 4, we can see that the Fast Sweeping method has a similar computational error as the Fast Marching method (less than 0.06%). We also compute the cross-correlation coefficient

$$\rho\left(T_{ex},T_{ns}\right)=\frac{\mathrm{cov}\left(T_{ex},T_{ns}\right)}{\sigma_{T_{ex}}\sigma_{T_{ns}}},$$ where $\mathrm{cov}\left(T_{ex},T_{ns}\right)$ represents the covariance of T_{ex} and T_{ns}; $\sigma_{T_{ex}}$ and $\sigma_{T_{ns}}$ are the standard deviations of T_{ex} and T_{ns}, respectively. The values of cross-correlation coefficient between 0 and 1 indicate the degree of correlation between T_{ex} and T_{ns}. The larger the cross-correlation coefficient, the higher the similarity between T_{ex} and T_{ns}. For the real part of the complex-valued traveltime, the cross-correlation coefficients are equal to 1 for the exact solution with the Fast Marching and Fast Sweeping methods, respectively. For the imaginary part, the cross-correlation coefficients are 0.9998 and 0.9998 for the exact solution with the Fast Marching and Fast Sweeping methods, respectively. The values of cross-correlation coefficients indicate that the Fast Marching method provides the same numerical accuracy as the Fast Sweeping method does.

SEG/Hess attenuating VTI model (Model 2)

Here, we use the modified SEG/Hess VTI model by adding attenuation (Fig. 5). The source is located at the center of the model with the dimensions $3.0km \times 1.25km$ and grid size $5m$. Fig. 6 demonstrates that the Fast Sweeping method is as stable and accurate as the Fast Marching method in complex media. Fig. 7 shows the differences $diff=\dfrac{\left|T_{fm}-T_{fw}\right|}{T_{fm}}$ are calculated for the (a) real and (b) imaginary parts of traveltimes obtained from the Fast Marching method (T_{fm}) and the Fast Sweeping method (T_{fw}), respectively. The differences are mostly deserved with substantial velocity changes.

To compare the computational efficiencies of the two methods, we ran our model tests on a laptop (Dell Inspiron 15-5555 with 8 GB Ram and AMD A8 Processor). Table 1 shows the computational times of the Fast Sweeping method and the Fast Marching method in both models (Model 1 and Model 2). Compared with the Fast Marching method, the Fast Sweeping method can save more than 70% of the computational times.

Table 1. Computational times of two numerical methods in Model 1 and Model 2.

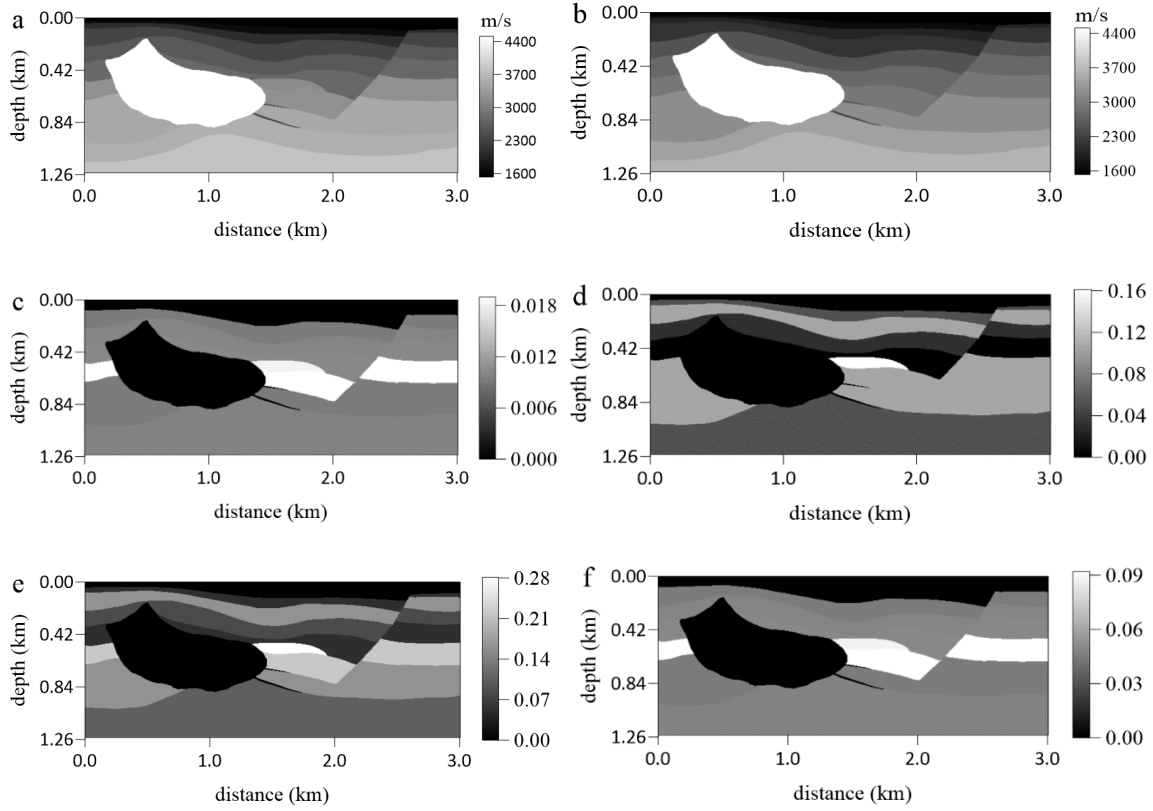| Running time (S)	Fast marching	Fast sweeping
Model-1	996	148
Model-2	2545.28	667.39

Fig. 5. SEG/Hess 2D attenuative VTI model (Model 2). (a) The normal moveout velocity v_n , (b) the P-wave vertical velocity v_p , (c) the P-wave attenuation coefficient A_{p0} , (d) Thomsen-style parameter δ_q , (e) Thomsen-style parameter ε_q , and (f) the anellipticity parameter η. The source is located at the center of the model with the dimensions $3.0km \times 1.25km$ and grid size 5 m.

CONCLUSIONS

The Fast Sweeping method and the Fast Marching method have been widely used in the first-arrival traveltime calculation. In this paper, we successfully performed the two methods in viscoacoustic VTI media and compared them in terms of accuracy and efficiency. The numerical results can demonstrate that the two numerical methods are stable and applicable for calculating the accurate first-arrival P-wave traveltime in the strongly heterogeneous attenuating VTI media. In addition, the Fast Sweeping method shows the same accuracy and stability as the Fast Marching method but more efficient. The factorization method reduces the calculation errors near the source and significantly improves the stability of first-arrival traveltime calculation.
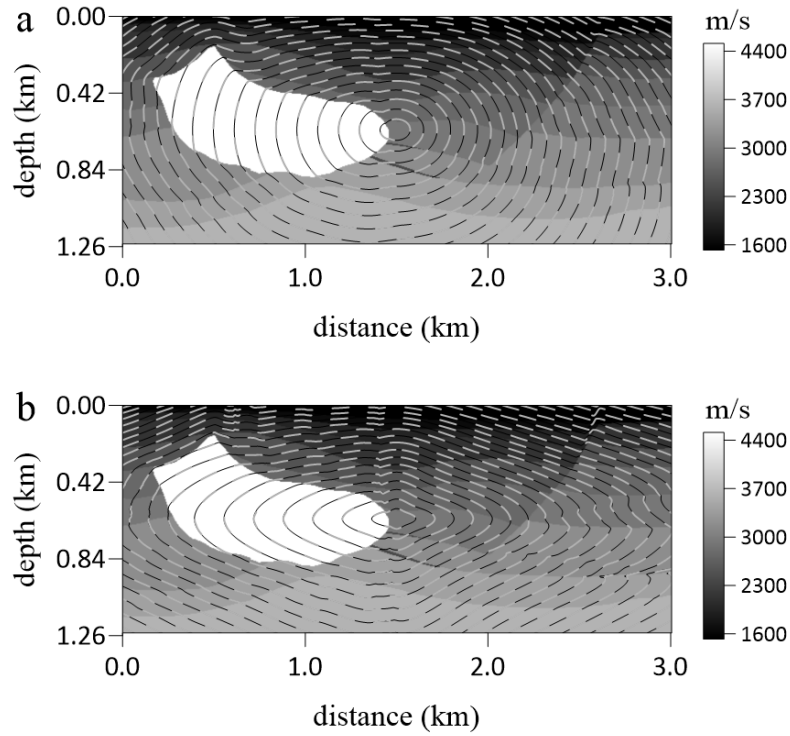
Fig. 6. Contours of the (a) real and (b) imaginary parts of the complex-valued traveltimes for Model 2 calculated from the Fast Marching method (gray dashed line) and the Fast Sweeping method (black solid line).
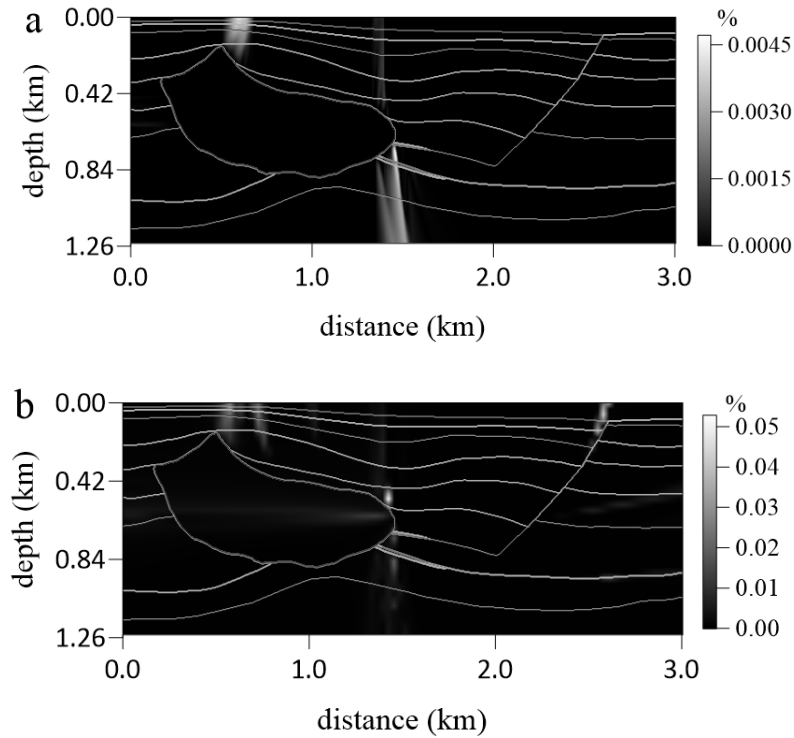

Fig. 7. The differences between the (a) real and (b) imaginary parts of the traveltimes calculated for Model 2 from the Fast Marching method and the Fast Sweeping method .

ACKNOWLEDGEMENTS

REFERENCES

Alkhalifah, T. and Fomel, S., 2001. Implementing the fast marching eikonal solver: spherical versus Cartesian coordinates. Geophysical Prospecting, 49(2), 165-178.

Alkhalifah, T., 2000. An acoustic wave equation for anisotropic media. Geophysics, 65: 1239-1250.

Babuska, V. and Cara, M., 1991. Seismic anisotropy in the Earth (Vol. 10). Springer Science & Business Media, Berlin.

Bai, T. and Tsvankin, I., 2019. Source-independent waveform inversion for attenuation estimation in anisotropic media. Geophys. Prosp., 67: 2343-2357.

Bai, T., Tsvankin, I. and Wu, X., 2017. Waveform inversion for attenuation estimation in anisotropic media. Geophysics, 82(4): WA83-WA93.

Blackman, D.K., Kendall, J.M., Dawson, P.R., Wenk, H.R., Boyce, D. and Morgan, J.P., 1996. Teleseismic imaging of subaxial flow at mid-ocean ridges: Traveltime effects of anisotropic mineral texture in the mantle. Geophys. J. Internat., 127: 415-426.

Červený, V. and Pšencík, I., 2009. Perturbation Hamiltonians in heterogeneous anisotropic weakly dissipative media. Geophys. J. Internat., 178: 939-949.

Červený, V., 2005. Seismic Ray Theory. Cambridge University Press, Cambridge.

Chichinina, T., Sabinin, V. and Ronquillo-Jarillo, G., 2006. QVOA analysis: P-wave attenuation anisotropy for fracture characterization. Geophysics, 71(3): C37-C48.

Cristiani, E., 2009. A fast marching method for Hamilton-Jacobi equations modeling monotone front propagations. Journal of Scientific Computing, 39(2), 189-205.

Fomel, S., Luo, S. and Zhao, H., 2009. Fast sweeping method for the factored eikonal equation. Journal of Computational Physics, 228(17), 6440-6455.

Guo, P. and McMechan, G.A., 2017. Sensitivity of 3D 3C synthetic seismograms to anisotropic attenuation and velocity in reservoir models. Geophysics, 82(2), T79-T95.

Hao, Q. and Alkhalifah, T., 2017a. An acoustic eikonal equation for attenuating transversely isotropic media with a vertical symmetry axis. Geophysics, 82(1): C9-C20.

Hao, Q. and Alkhalifah, T., 2017b. An acoustic eikonal equation for attenuating orthorhombic media. Geophysics, 82(4), WA67-WA81.

Hao, Q. and Alkhalifah, T., 2019. Viscoacoustic anisotropic wave equations. Geophysics, 84(6): C323-C337.

Hao, Q., Waheed, U. and Alkhalifah, T., 2018. A Fast Sweeping Scheme for P-wave Traveltimes in Attenuating VTI Media. Extended Abstr., 80th EAGE Conf., Copenhagen.

Kendall, J.M., 1994. Teleseismic arrivals at a mid-ocean ridge: Effects of mantle melt and anisotropy. Geophys. Res. Lett., 21: 301-304.

Konukoglu, E., Sermesant, M., Clatz, O., Peyrat, J.M., Delingette, H. and Ayache, N., 2007. A recursive anisotropic fast marching approach to reaction diffusion equation: Application to tumor growth modeling. In: Biennial Internat. Conf. Informat. Process. Medic. Imag. (687-699). Springer Verlag, Berlin, Heidelberg.

Lan, H. and Zhang, Z., 2013. Topography-dependent eikonal equation and its solver for calculating first-arrival traveltimes with an irregular surface. Geophys. J. Internat., 193: 1010-1026.

Lan, H., Zhang, Z., Xu, T., Bai, Z. and Liang, K., 2012. A comparative study on the fast marching and fast sweeping methods in the calculation of first-arrival traveltime field. Progr. Geophys. (in Chinese), 27: 1863-1870.

Luo, S. and Qian, J., 2012. Fast sweeping methods for factored anisotropic eikonal equations: multiplicative and additive factors. J. Sci. Comput., 52: 360-382.

Popovici, A.M. and Sethian, J.A., 2002. 3-D imaging using higher order fast marching traveltimes. Geophysics, 67: 604-609.

Qian, J., Zhang, Y. and Zhao, H., 2007. A fast sweeping method for static convex Hamilton–Jacobi equations. J. Sci. Comput., 31: 237-271.

Qin, F., Luo, Y., Olsen, K.B., Cai, W. and Schuster, G.T., 1992. Finite-difference solution of the eikonal equation along expanding wavefronts. Geophysics, 57: 478-487.

Qin, F., Luo, Y., Olsen, K.B., Cai, W. and Schuster, G.T., 1992. Finite-difference solution of the eikonal equation along expanding wavefronts. Geophysics, 57: 378-504.

Schoenberg, M. and Sayers, C.M., 1995. Seismic anisotropy of fractured rock. Geophysics, 60: 204-211.

Sethian, J.A. and Vladimirsky, A., 2003. Ordered upwind methods for static Hamilton-Jacobi equations: Theory and algorithms. SIAM J. Numer. Analys, 41: 325-363.

Sethian, J.A., 1996. A fast marching level set method for monotonically advancing fronts. Proc. Nat. Acad. Sci., 93: 1591-1595.

Thomsen, L., 1986. Weak elastic anisotropy. Geophysics, 51: 1954-1966.

Tsvankin, I., 2012, Seismic Signatures and Analysis of Reflection Data in Anisotropic Media, 3rd ed. SEG, Tulsa, OK.

Tsvankin, I. and Grechka, V., 2011. Seismology of azimuthally anisotropic media and seismic fracture characterization. Society of Exploration Geophysicists.

Vavryčuk, V., 2007. Ray velocity and ray attenuation in homogeneous anisotropic viscoelastic media. Geophysics, 72(6), D119-D127.

Vavryčuk, V., 2010. Behaviour of rays at interfaces in anisotropic viscoelastic media. Geophys. J. Internat., 181: 1665-1677.

Vidale, J., 1988. Finite-difference calculation of travel times. Bull. Seismol. Soc. Am., 78: 2062-2076.

Waheed, U.B. and Alkhalifah, T., 2017. A fast sweeping algorithm for accurate solution of the tilted transversely isotropic eikonal equation using factorization. Geophysics, 82(6): WB1-WB8.

Waheed, U.B., Yarman, C.E. and Flagg, G., 2015. An iterative, fast-sweeping-based eikonal solver for 3D tilted anisotropic media. Geophysics, 80(3): C49-C58.

Xu, T., Xu, G., Gao, E., Li, Y., Jiang, X. and Luo, K., 2006. Block modeling and segmentally iterative ray tracing in complex 3D media. Geophysics, 71(3): T41-T51.

Zhao, H., 2005. A fast sweeping method for eikonal equations. Mathemat. Computat., 74: 603-627.

Zhu, Y. and Tsvankin, I., 2006. Plane-wave propagation in attenuative transversely isotropic media. Geophysics, 71(2): T17-T30.